

DeepPoint: A Deep Learning Model for 3D Reconstruction in Point Clouds via mmWave Radar

Yue Sun¹, Honggang Zhang², Zhuoming Huang³, and Benyuan Liu⁴

Abstract—Recent research has shown that mmWave radar sensing is effective for object detection in low visibility environments, which makes it an ideal technique in autonomous navigation systems such as autonomous vehicles. However, due to the characteristics of radar signals such as sparsity, low resolution, specularity, and high noise, it is still quite challenging to reconstruct 3D object shapes via mmWave radar sensing. Built on our recent proposed 3DRIMR (3D Reconstruction and Imaging via mmWave Radar), we introduce in this paper DeepPoint, a deep learning model that generates 3D objects in point cloud format that significantly outperforms the original 3DRIMR design. The model adopts a conditional Generative Adversarial Network (GAN) based deep neural network architecture. It takes as input the 2D depth images of an object generated by 3DRIMR’s Stage 1, and outputs smooth and dense 3D point clouds of the object. The model consists of a novel generator network that utilizes a sequence of DeepPoint blocks or layers to extract essential features of the union of multiple rough and sparse input point clouds of an object when observed from various viewpoints, given that those input point clouds may contain many incorrect points due to the imperfect generation process of 3DRIMR’s Stage 1. The design of DeepPoint adopts a deep structure to capture the global features of input point clouds, and it relies on an optimally chosen number of DeepPoint blocks and skip connections to achieve performance improvement over the original 3DRIMR design. Our experiments have demonstrated that this model significantly outperforms the original 3DRIMR and other standard techniques in reconstructing 3D objects.

I. INTRODUCTION

The advantage of Millimeter Wave (mmWave) radar in object sensing in low visibility environment has been actively studied recently in applying it in autonomous vehicles [1] and search/rescue in high risk areas [2]. However further application of mmWave radar in object imaging and reconstruction is quite difficult due to the characteristics of mmWave radar signals such as low resolution, sparsity, and high noise due to multi-path and specularity. Recent work [1]–[3] attempt to design deep learning systems to generate 2D depth images based on mmWave radar signals. 3DRIMR [4] further introduces a design that generates 3D object shapes based on mmWave radar, but the end results are still not satisfactory.

In this paper, we introduce DeepPoint, a deep learning model that generates 3D objects in dense and smooth point

clouds based on the union of multiple rough and sparse input point clouds, which are directly converted from the 2D depth images generated by the Stage 1 of 3DRIMR which takes raw radar data as input. The training of DeepPoint follows conditional GAN architecture, and it significantly outperforms the original 3DRIMR design.

The 3DRIMR [4] architecture consists of two stages, and each has a generator network. Stage 1’s generator network G_{r2i} takes 3D radar intensity data as input and generates 2D depth images; Stage 2’s generator network G_{p2p} takes as input a set of multiple 2D depth images and outputs the 3D shape of the object in the format of point cloud. Each stage’s generator network is jointly trained with a separate discriminator network, using conditional GAN architecture. The design rationale for 3DRIMR architecture is to combine the advantages of Convolutional Neural Network (CNN)’s convolutional operation and the efficiency of point cloud representation of 3D objects, as the former can capture detailed local neighborhood structure of a 3D object, and the latter is more efficient and of higher resolution than 3D shape representation via voxelization.

Even though 3DRIMR has shown promising results, its Stage 2’s generator network design is still not quite satisfactory. Specifically, the edges of generated 3D objects are still blurry and the points of an object’s point cloud tend to evenly distributed in space which do not give a clear sharp shape structure. DeepPoint introduced in this paper replaces the Stage 2 of the original 3DRIMR, and it significantly outperforms 3DRIMR both quantitatively and visually.

Our major contributions are as follows:

- 1) DeepPoint, a novel generator network that can generate smooth and dense point cloud representation of a 3D object based on the union of multiple rough and sparse point clouds directly converted from the 2D depth images derived from raw mmWave radar sensor data. The generator network utilizes a sequence of DeepPoint blocks or layers to extract essential features of those input point clouds of an object when observed from various viewpoints, even though those input point clouds may contain many incorrect points due to the imperfect generation process of 3DRIMR’s Stage 1.
- 2) Novel designs such as a conditional GAN architecture design for the training of DeepPoint, an optimally chosen number of layers and skip connection. Those designs have resulted in the performance improvement over the original 3DRIMR.
- 3) An improved 3DRIMR system implementation that can conduct fast 3D object reconstruction by using a com-

¹Yue Sun is in the Department of Computer Science, UMass Boston, USA. Yue.Sun001@umb.edu

²Honggang Zhang is in the Department of Engineering, UMass Boston, USA. Honggang.Zhang@umb.edu

³Zhuoming Huang is in the Department of Engineering, UMass Boston, USA. Zhuoming.Huang001@umb.edu

⁴Benyuan Liu is in the Department of Computer Science, UMass Lowell, USA. bliu@cs.uml.edu

modity mmWave radar sensor, instead of a slow full-scale SAR scan. The whole system takes advantage of convolutional operation and point cloud based neural network for efficient 3D shape generation with detailed geometry.

In the rest of the paper, we briefly discuss related work and preliminaries in Sections II and III. Then we discuss the design of DeepPoint model in Section IV. Experiment results are given in Section V. Finally the paper concludes in Section VI.

II. RELATED WORK

Frequency Modulated Continuous Wave (FMCW) Millimeter Wave (mmWave) radar sensing has been an active research area in recent years, especially in applications such as person/gesture identification [5], [6], car detection/imaging [1], and environment sensing [2], [3]. Usually Synthetic Aperture Radar (SAR) is used in data collection for high resolution, e.g., [7]–[10].

This paper is built on our recent work [4] on applying mmWave radar for 3D object reconstruction, in which we proposed 3DRIMR system. The deep neural network model proposed in this paper completely replaces the model in the Stage 2 of 3DRIMR, and this new model significantly outperforms the original 3DRIMR. There have been a few recent work on mmWave radar based imaging, mapping, and 3D object reconstruction [1]–[3], [11], [12]. Our work is inspired by their promising research results, and due to the low cost and small form factor of commodity mmWave radar sensors, we plan to develop a simple and fast 3D reconstruction system to be attached in our UAV SLAM system [13] for search and rescue in dangerous environment.

Besides radar signals, vision community has also been working on learning-based 3D object shape reconstruction [14]–[17], most of which use voxels to represent 3D objects. Our proposed neural network model uses point cloud as a format for 3D objects to capture detailed geometric information with efficient memory and computation performance.

PointNet structure is utilized in PCN [11], which uses point cloud to reconstruct 3D object shapes, and this structure inspires us to design our model. The novelty of our model is that it has a deeper structure than PCN and skip connections are used for better capture of objects’ edges and shapes. In addition, our work adopts a conditional GAN architecture to jointly train a generator and a discriminator for better performance.

III. PRELIMINARIES

A. FMCW Millimeter Wave Radar Sensing and Imaging

Similar to [4], we use Frequency Modulated Continuous Wave (FMCW) mmWave radar sensor [18] signals to reconstruct 3D object shapes. Three Fast Fourier Transforms (FFTs) are conducted on received waveforms to generate 3D heatmaps or intensity maps of the space that represent the energy or radar intensity per voxel, written as $x(\phi, \theta, \rho)$. Note that ϕ , θ , and ρ represent azimuth angle, elevation angle, and range respectively. Same as in [4], we use IWR6843ISK [19]

operating at 60 GHz frequency, and for high resolution radar signals, we adopt the Synthetic Aperture Radar (SAR) operation. Unlike data from LiDAR and camera sensor, mmWave radar sensors can only give us sparse, low resolution, and highly noisy data. Partially, incorrect ghost points in radar signals can be generated due to multi-path effect. Reference [1]–[3] give more detailed discussion on FMCW mmWave radar sensing.

B. Representation of 3D Objects

In this work, we adopt point cloud format to represent 3D objects. Even though point cloud format is a standard representation of 3D objects and it is used in learning-based 3D reconstruction, e.g., [12], [20], [21], but CNN convolutional operation cannot be directly applied to a point cloud set as it is essentially an unordered point set. Furthermore, the point cloud of an object that is directly generated by raw radar signals is not a good choice to reconstruct the object due to the radar signal’s low resolution, being sparse, and with incorrect ghost points due to multi-path effect. Besides point clouds, voxel representations can also be used in 3D reconstruction [22]–[25], and the advantage of such representation is that 3D CNN convolutional operations can be applied to it. In addition, mesh representations of 3D objects are also used in existing work [26], [27]. However these two representation formats are limited by memory and computation cost.

C. Review of 3DRIMR Architecture

This paper introduces DeepPoint as the generator and discriminator networks of the Stage 2 of 3DRIMR to generate smooth and dense point clouds. For completeness, we now briefly review 3DRIMR architecture.

3DRIMR consists of two back-to-back generator networks \mathbf{G}_{r2i} and \mathbf{G}_{p2p} . In Stage 1, \mathbf{G}_{r2i} receives a 3D radar energy intensity map of an object and outputs a 2D depth image of the object. We let a mmWave radar sensor scans an object from multiple viewpoints to get multiple 3D energy maps. Then \mathbf{G}_{r2i} generates multiple 2D depth images of the object. The Stage 2 of 3DRIMR first pre-processes these images to get multiple coarse point clouds of the object, which are used as input to \mathbf{G}_{p2p} to generate a single point cloud of the object. A conditional GAN architecture is designed for 3DRIMR’s training. That is, two discriminator networks \mathbf{D}_{r2i} and \mathbf{D}_{p2p} that are jointly trained together with their corresponding generator networks.

Let m_r denote a 3D radar intensity map of an object captured from a viewpoint, and let g_{2d} be a ground truth 2D depth image of the same object captured from the same viewpoint. \mathbf{G}_{r2i} generates \hat{g}_{2d} that predicts or estimates g_{2d} given m_r . If there are k different viewpoints v_1, \dots, v_k , generator \mathbf{G}_{r2i} predicts their corresponding 2D depth images $\{\hat{g}_{2d,i} | i = 1, \dots, k\}$. Each $\hat{g}_{2d,i}$ can be directly converted to a coarse and sparse 3D point cloud. Then we can have k coarse point clouds $\{P_{r,i} | i = 1, \dots, k\}$ of the object. The Stage 2 of 3DRIMR unions the k coarse point clouds to form an initial estimated coarse point cloud of the object, denoted as

P_r , which is a set of 3D points $\{p_j|j = 1, \dots, n\}$. Generator $\mathbf{G}_{\mathbf{p2p}}$ takes P_r as input, and predicts a dense, smooth, and accurate point cloud \hat{P}_r . Note that since the prediction of $\mathbf{G}_{\mathbf{r2i}}$ may not be completely correct, a coarse P_r may likely contain many missing or even incorrect points.

The Stage 1's design of 3DRIMR can be found in [4]. Next we discuss our proposed DeepPoint as the network model in the Stage 2 of 3DRIMR.

IV. DEEPPPOINT DESIGN

A. Overview

DeepPoint is a generative model to generate a smooth and dense 3D point cloud of an object from the union of multiple coarse point clouds, which are directly converted from 2D depth images of the object observed from different viewpoints. Since those 2D depth images are generated from raw radar energy maps, the union of their converted point clouds may contain many incorrect points due to the imperfect image generation process. DeepPoint's generator network is able to correct those incorrect points and generate a smooth and dense point cloud. This generator can be used as the network in the Stage 2 of 3DRIMR, and it also can be used as an independent network model that works on any rough and sparse input point clouds that contains incorrect points.

The training of DeepPoint is a conditional GAN architecture, as shown in Fig. 1. DeepPoint's generator network $\mathbf{G}_{\mathbf{p2p}}$ aims at generating a point cloud of an object with continuous and smooth contour \hat{P}_r , from P_r , a union of k separate coarse point clouds observed from k viewpoints of the object $\{P_{r,i}|i = 1, \dots, k\}$.

B. Generator $\mathbf{G}_{\mathbf{p2p}}$

Generator $\mathbf{G}_{\mathbf{p2p}}$'s input P_r and output $\hat{P}_r = \mathbf{G}_{\mathbf{p2p}}(P_r)$ are 3D point clouds represented as $n \times 3$ matrices, with each row being the 3D Cartesian coordinate (x, y, z) of a point. However, different from the Stage 2's generator in [4], the input and output point clouds in our work should have the same number of points due to the use of Earth Mover's Distance (EMD) in the loss function design for the training of the generator network.

Generator $\mathbf{G}_{\mathbf{p2p}}$ consists of a series of blocks that expand an input point cloud P_r into a high dimensional feature and then shrink it into 3-dimensional outputs \hat{P}_r . These blocks are referred to as DeepPoint Block, and their designs are inspired by PointNet structure. During the training, a discriminator $\mathbf{D}_{\mathbf{p2p}}$ takes (P_r, P_{true}) or (P_r, \hat{P}_r) pairs and outputs a score to indicate the difference between them.

As shown left part of Fig. 1, the generator takes the input P_r , and converts it into a high-dimensional point feature matrix after passing first 2 DeepPoint blocks, and then decreases the dimension of feature matrices through the following 3 DeepPoint blocks, and finally outputs a new set of 3-dimensional matrix \hat{P}_r , which represents the Cartesian coordinate (x, y, z) of a point of the predicted point cloud.

The detailed structure of each DeepPoint block is shown in the bottom dotted box of Generator in Fig. 1. It first passes

the raw input into a shared MLP, and then concatenates the raw input, i.e., the Cartesian coordinate (x, y, z) of the input point cloud, to form a point feature matrix F_{P_r} with each row representing the local feature of a corresponding point. Then, it applies a point-wise maxpooling on F_{P_r} and extracts a global feature vector g_{P_r} . To produce a complete point cloud for an object, we need both local and global features, therefore, we concatenate the global feature g_{P_r} with each of the point features f_i and form another matrix F'_{P_r} .

Remarks. Note that there are two major differences between the proposed generator network and the generator in Stage 2 of 3DMIMR [4]. First, the proposed generator is "deeper" than the generator of 3DMIMR as ours has more layers of DeepPoint blocks. Second, 3DMIMR uses fully connected layers and apply reshape operation to derive output point cloud from a high-dimensional global feature vector, which can only get an rough overall shape without many fine, local, and detailed characteristics. However, our new generator network design generates an output point cloud from both local and global features and hence can generate fine, local and detailed characteristics of an object.

C. Discriminator $\mathbf{D}_{\mathbf{p2p}}$

We design an improved discriminator with two-stream inputs, as shown in Fig. 1. The inputs pass through a simple shared MLP and get expanded into higher dimensional matrices. A point-wise max pooling and an average pooling are used to extract two global feature vectors. Then the two global feature vectors are concatenated to form final global features, which are further concatenated and fed into two fully connected layers to derive a score. The score is used to indicate whether the input is real or fake, i.e., generated point cloud.

D. Loss Function

When training the generator network, we concurrently train $\mathbf{D}_{\mathbf{p2p}}$ to minimize $\mathcal{L}_{\mathbf{D}_{\mathbf{p2p}}}$, and train $\mathbf{G}_{\mathbf{p2p}}$ to minimize $\mathcal{L}_{\mathbf{G}_{\mathbf{p2p}}}$. $\mathcal{L}_{\mathbf{D}_{\mathbf{p2p}}}$ is calculated as the mean MSE (Mean Square Error) of $\mathbf{D}_{\mathbf{p2p}}$'s prediction error. The loss function of generator $\mathcal{L}_{\mathbf{G}_{\mathbf{p2p}}}$ is a weighted sum, consisting of $\mathcal{L}_{GAN}(\mathbf{G}_{\mathbf{p2p}})$, Chamfer loss \mathcal{L}_{cf} between predicted point clouds and the ground truth, and EMD [11] loss $\mathcal{L}_{emd}(\mathbf{G}_{\mathbf{p2p}})$.

Note that Chamfer distance [11] calculates the average closest distance between input and output points. The symmetric version of it is defined as:

$$d_{cf}(S_1, S_2) = \frac{1}{|S_1|} \sum_{x \in S_1} \min_{y \in S_2} \|x - y\|_2 + \frac{1}{|S_2|} \sum_{y \in S_2} \min_{x \in S_1} \|y - x\|_2 \quad (1)$$

Then, Chamfer loss is defined as:

$$\mathcal{L}_{cf}(\mathbf{G}_{\mathbf{p2p}}) = d_{cf}(\hat{P}_r, P_{true}) \quad (2)$$

In addition, Earth Mover's Distance (EMD) [11] can find a bijection $\phi : S_1 \rightarrow S_2$, which can minimize the average distance between pairs of corresponding points. The equation of EMD is:

$$d_{emd}(S_1, S_2) = \min_{\phi: S_1 \rightarrow S_2} \frac{1}{|S_1|} \sum_{x \in S_1} \|x - \phi(x)\|_2 \quad (3)$$

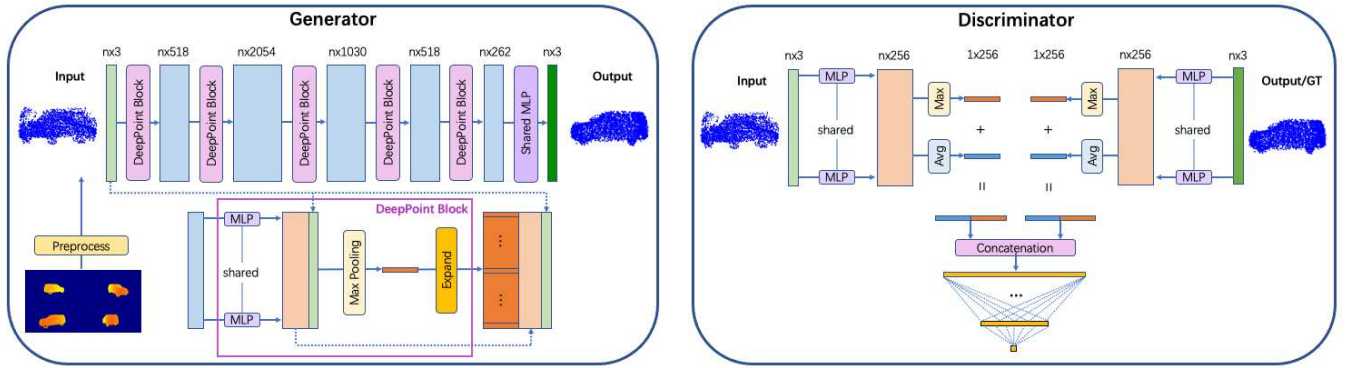


Fig. 1: DeepPoint architecture proposed in this paper. The system first pre-processes multiple 2D depth images of an object to get multiple coarse and sparse point clouds, which may contain many incorrect points. Those depth images are generated for the same object but viewed from four different viewpoints. Combining those coarse point clouds we can derive a single coarse point cloud, which is used as the input of the generator $\mathbf{G}_{\mathbf{p2p}}$ of DeepPoint. The generator of DeepPoint outputs a dense and smooth point cloud representation of the object. A conditional GAN architecture is used to train both generator $\mathbf{G}_{\mathbf{p2p}}$ and discriminator $\mathbf{D}_{\mathbf{p2p}}$ jointly.

In our case, EMD loss is calculated as:

$$\mathcal{L}_{emd}(\mathbf{G}_{\mathbf{p2p}}) = d_{emd}(\hat{P}_r, P_{true}) \quad (4)$$

$\mathcal{L}_{\mathbf{G}_{\mathbf{p2p}}}$ is given by Eqn. (5). Note that $\lambda_{d_{cf}}$ and $\lambda_{d_{emd}}$ are hand-tuned to 100 and 1 respectively in our experiments.

$$\begin{aligned} \mathcal{L}_{\mathbf{G}_{\mathbf{p2p}}} = & \mathcal{L}_{GAN}(\mathbf{G}_{\mathbf{p2p}}) + \lambda_{d_{cf}} \mathcal{L}_{cf}(\mathbf{G}_{\mathbf{p2p}}) \\ & + \lambda_{d_{emd}} \mathcal{L}_{emd}(\mathbf{G}_{\mathbf{p2p}}) \end{aligned} \quad (5)$$

V. IMPLEMENTATION AND EXPERIMENTS

We implement DeepPoint and use it as Stage 2’s generator network of 3DRIMR [4] system. The system first generates 2D depth images from 3D radar intensity maps from multiple views of an object, and then passes these output depth images to the generator network of DeepPoint to produce a 3D point cloud of the object. We now present our experiment results in this section.

A. Datasets

We conduct experiments on cars with average size of $445\text{cm} \times 175\text{cm} \times 158\text{cm}$. The input data to the proposed the generator network is the output depth images produced by 3DRIMR’s Stage 1. We follow a procedure that is similar to 3DRIMR [4], to generate ground truth point clouds. Fig. 2 shows an example scene.

B. Model Training and Testing

We use the 2D depth images generated in the Stage 1 of 3DRIMR to form a dataset of coarse and sparse point clouds, which includes 1600 point clouds with 200 point clouds of each car model. We train the proposed generator network and discriminator network for 200 epochs using 1520 point clouds with batch size 4. The learning rate for the first 100 epochs is 2×10^{-4} and linearly decreases to 0 in the rest 100 epochs. Then we test the generator network using the remaining 80 point clouds. Fig. 3 shows some example results of generated 2D depth images from the Stage 1 of 3DRIMR.

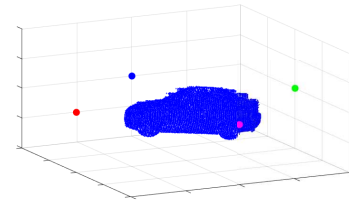


Fig. 2: An example scene of a car.

Method	CD		EMD		F-score	
	avg.	std.	avg.	std.	avg.	std.
3DRIMR	7.89	4.11	-	-	8.41	3.22
1-Block, w/o sc	10.10	4.49	5.01	4.24	8.40	3.40
1-Block	9.75	4.00	4.56	3.96	8.47	3.44
2-Block	9.40	4.70	4.83	4.84	9.40	4.22
5-Block	7.79	4.37	4.40	4.49	13.10	5.97
7-Block	7.68	4.15	4.53	4.19	13.23	6.34
7-Block + 3sc	9.13	4.55	4.66	3.88	10.70	4.90

TABLE I: Quantitative results under different setups. Note that the units of CD and EMD in this table are cm, and the magnitude of F-score is 10^{-2} .

C. Evaluation Results

In this section, we compare our generator network performance with the original 3DRIMR [4] since both of them aim at reconstructing objects’ 3D point clouds from sparse radar data. We also validate our design choices for generator and discriminator networks by controlled experiments. We conduct experiments by varying the number of layers, i.e., DeepPoint blocks, in our proposed generator network model. Specifically, as shown in Table I, we tested 1, 2, 5 and 7 layers of DeepPoint blocks in our generator network.

1) *Comparison with 3DRIMR:* In Table I, we can see the our generator network with 5-Block and 7-Block significantly outperforms the original 3DRIMR in terms of

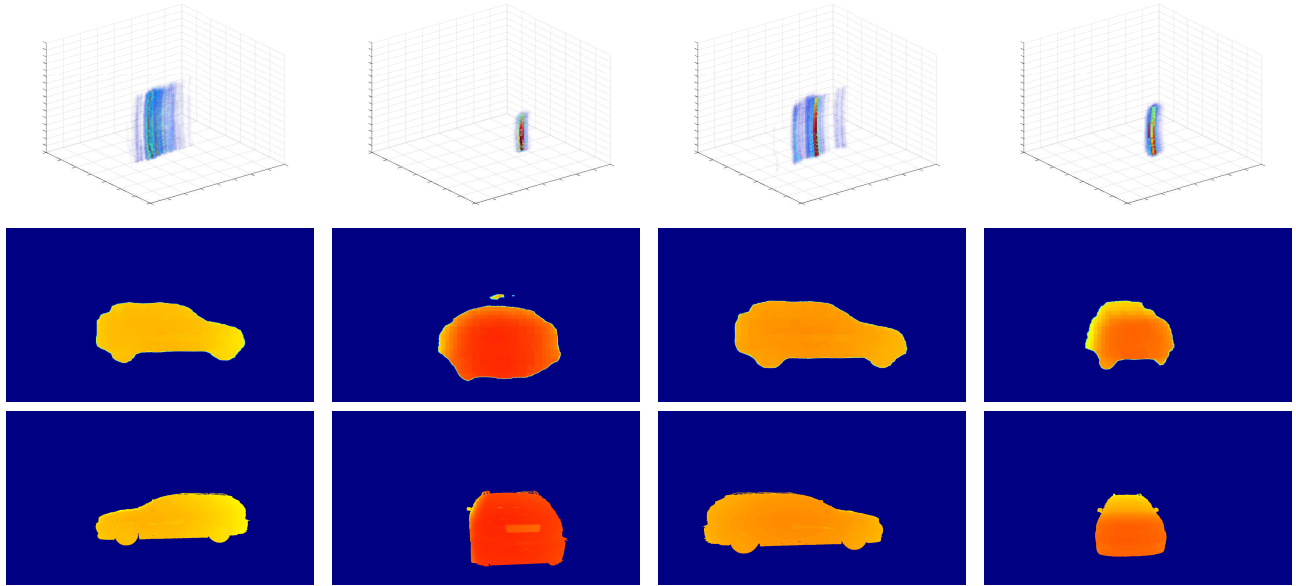


Fig. 3: Example results of generated 2D depth images from the Stage 1 of 3DRIMR. The generated images are used as inputs to DeepPoint (which is used as the Stage 2 of 3DRIMR). The 1st row shows the 3D radar intensity data from 2 snapshots only. The 2nd row shows the outputs from 3DRIMR’s Stage 1. The 3rd row shows the ground truth depth images.

both Chamfer Distance (CD) and F-score. Note that EMD results are not available for 3DRIMR. In addition, Fig. 4 demonstrates that the visual improvement of output point clouds is even more obvious. This is because 3DRIMR can only reconstruct an overall shape of the object whereas our proposed generator network can recover more fine details of the shape, e.g., correct orientation, and the shapes of wheels of the car. This significant improvement is due to the “deeper” structure of the generator network, the optimal number of DeepPoint blocks, the introduction of skip connections, and the use of a more efficient training loss metric, i.e., Earth Mover’s Distance (EMD).

2) *Performances of different layers of DeepPoint Blocks:* The DeepPoint blocks in our generator network first expand each input point’s dimension and then shrink them back to 3 to get each output point’s coordinates. The more such DeepPoint blocks means the generator network is “deeper”, which seems achieve better performance. However, this is not always true. There exists an optimal number of layers. As shown in Fig. 5, the performance of our generator improves with the number of DeepPoint blocks increasing, i.e., CD decreases from 9.8 cm to 7.8 cm and EMD decreases from 4.6 cm to 4.4 cm as the number of DeepPoint Blocks increases from 1 to 5. Correspondingly, F-score is even improved around 55%. However, after the number of DeepPoint blocks reaches an upper bound, say 5 in our experiment, further increasing the number of DeepPoint blocks to 7 can no longer largely improve the performance. We can see that all these 3 evaluation metrics are very similar in these two cases.

3) *Skip Connections in Generator Network:* As shown in Fig. 1, we can see inside each DeepPoint block, we concatenate the raw input points’ Cartesian coordinates with

Method	CD		EMD		F-score	
	avg.	std.	avg.	std.	avg.	std.
Mix Pooling	9.75	4.00	4.56	3.96	8.47	3.44
Max Pooling	10.52	4.80	4.79	4.33	7.29	2.71
Average Pooling	10.28	4.11	4.60	4.11	7.71	3.18

TABLE II: Quantitative Results of Stage 2 using different pooling methods in the discriminator. Note that the units of CD and EMD in this table are cm, and the magnitude of F-score is 10^{-2} .

feature matrix obtained by passing through the shared MLP to further form the point features. Our experiment results (e.g., Table I) clearly show that such skip connection design can improve the performance. However, blindly increasing skip connections will not always help. As shown in another experiment in which we build 3 more skip connections by concatenating the 1st and 7th point features, 2nd and 6th point features, and 3rd and 5th point features respectively. However, based on the results shown in Table I, we can see that with these additional skip connections, generator performs worse compared with the case without using them. In our future work, we will investigate an optimal placement of skip connections.

4) *Variants of Discriminator:* In our discriminator network design, we use mix pooling to extract the global feature vectors. Mix pooling means that we concatenate the feature vectors from both max pooling and average pooling. We compare the results of using max pooling, average pooling and mix pooling in the discriminator in Table II. Note that the generators in these 3 experiments are the same. Table II shows that mix pooling performs best among these three pooling methods, and max pooling falls a little behind average pooling method.

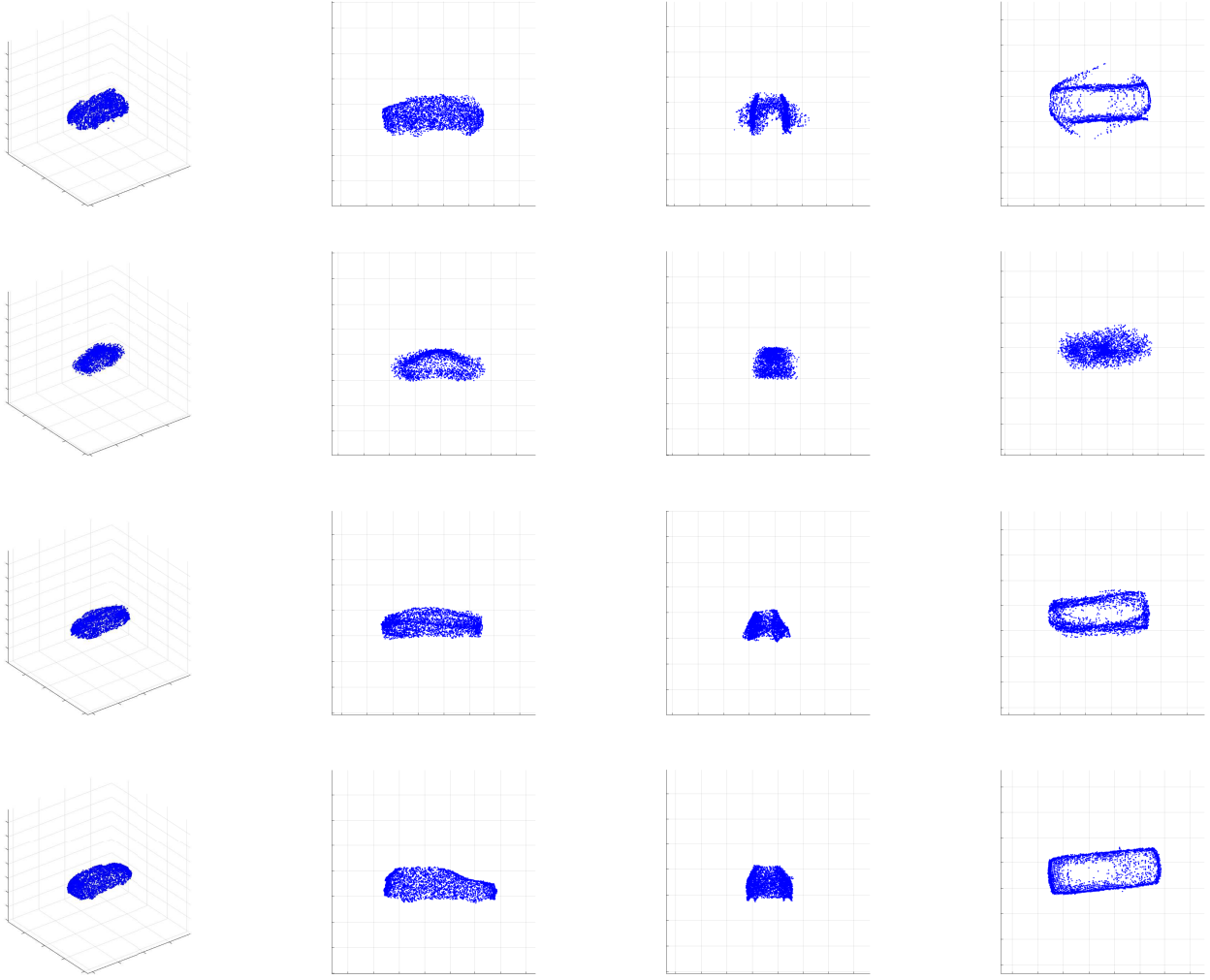


Fig. 4: Example experimental results of the proposed generator network. The 1st row shows the input point clouds of a car from different viewpoints (i.e., inputs to the generator network). The 2nd row shows the output point clouds of 3DRIMR. The 3rd row shows the output point clouds of DeepPoint. The 4th row shows the ground truth point clouds. Counting from the side, the 1st column lists point clouds shown in 3D space. The 2nd column lists the front views of point clouds. The 3rd column shows the side views of point clouds. The 4th column shows the top views of point clouds.

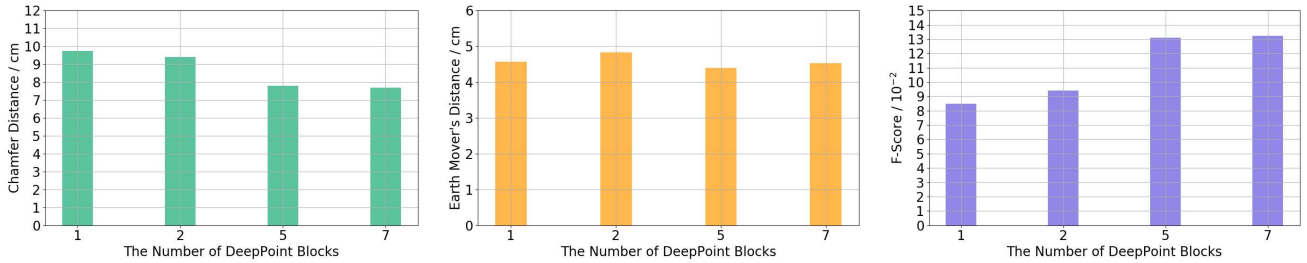


Fig. 5: Comparison of different numbers of DeepPoint blocks used in the design of the generator network.

VI. CONCLUSIONS AND FUTURE WORK

We have proposed DeepPoint, a deep learning model that generates 3D objects in smooth and dense point clouds. It utilizes a sequence of novel DeepPoint blocks to extract essential features of the union of multiple rough and sparse input point clouds of an object when observed from various viewpoints, even though the inputs contain many incorrect

points. It relies on a deep structure design, an optimally chosen number of DeepPoint blocks, and skip connections to achieve good 3D reconstruction performance. For future work, we will find the optimal placement of skip connections and introduce new techniques to improve the detailed geometry of generated point clouds. We will also conduct large scale experiments to improve our design.

REFERENCES

- [1] J. Guan, S. Madani, S. Jog, S. Gupta, and H. Hassanieh, "Through fog high-resolution imaging using millimeter wave radar," in *IEEE CVPR 2020*.
- [2] C. X. Lu, S. Rosa, P. Zhao, B. Wang, C. Chen, J. A. Stankovic, N. Trigoni, and A. Markham, "See through smoke: robust indoor mapping with low-cost mmwave radar," in *ACM MobiSys 2020*.
- [3] S. Fang and S. Nirjon, "Superrf: Enhanced 3d rf representation using stationary low-cost mmwave radar," in *Proc. of 2020 Intl Conf on Embedded Wireless Systems and Networks*.
- [4] Y. Sun, Z. Huang, H. Zhang, Z. Cao, and D. Xu, "3drimr: 3d reconstruction and imaging via mmwave radar based on deep learning," in *IEEE IPCCC, 2021*.
- [5] B. Vandersmissen, N. Knudde, A. Jalalvand, I. Couckuyt, A. Bourdoux, W. De Neve, and T. Dhaene, "Indoor person identification using a low-power fmcw radar," *IEEE Transactions on Geoscience and Remote Sensing*, vol. 56, no. 7, pp. 3941–3952, 2018.
- [6] X. Yang, J. Liu, Y. Chen, X. Guo, and Y. Xie, "Mu-id: Multi-user identification through gaits using millimeter wave radios," in *IEEE INFOCOM 2020*.
- [7] B. Mamandipoor, G. Malysa, A. Arbabian, U. Madhow, and K. Noujeim, "60 ghz synthetic aperture radar for short-range imaging: Theory and experiments," in *2014 48th Asilomar Conference on Signals, Systems and Computers*. IEEE, 2014, pp. 553–558.
- [8] E. National Academies of Sciences, Medicine *et al.*, *Airport Passenger Screening Using Millimeter Wave Machines: Compliance with Guidelines*. National Academies Press, 2018.
- [9] M. T. Ghasr, M. J. Horst, M. R. Dvorsky, and R. Zoughi, "Wideband microwave camera for real-time 3-d imaging," *IEEE Transactions on Antennas and Propagation*, vol. 65, no. 1, pp. 258–268, 2016.
- [10] D. M. Sheen, D. L. McMakin, and T. E. Hall, "Near field imaging at microwave and millimeter wave frequencies," in *2007 IEEE/MTT-S International Microwave Symposium*. IEEE, 2007, pp. 1693–1696.
- [11] W. Yuan, T. Khot, D. Held, C. Mertz, and M. Hebert, "Pcn: Point completion network," in *2018 International Conference on 3D Vision (3DV)*. IEEE, 2018, pp. 728–737.
- [12] C. R. Qi, H. Su, K. Mo, and L. J. Guibas, "Pointnet: Deep learning on point sets for 3d classification and segmentation," *arXiv preprint arXiv:1612.00593*, 2016.
- [13] Y. Sun, D. Xu, Z. Huang, H. Zhang, and X. Liang, "Lidaus: Localization of iot device via anchor uav slam," in *IEEE IPCCC 2020*.
- [14] B. Yang, H. Wen, S. Wang, R. Clark, A. Markham, and N. Trigoni, "3d object reconstruction from a single depth view with adversarial learning," in *IEEE International Conference on Computer Vision Workshops, 2017*.
- [15] A. Dai, C. Ruizhongtai Qi, and M. Nießner, "Shape completion using 3d-encoder-predictor cnns and shape synthesis," in *IEEE CVPR 2017*.
- [16] A. Sharma, O. Grau, and M. Fritz, "Vconv-dae: Deep volumetric shape learning without object labels," in *European Conference on Computer Vision*. Springer, 2016, pp. 236–250.
- [17] E. J. Smith and D. Meger, "Improved adversarial systems for 3d object generation and reconstruction," in *Conference on Robot Learning*. PMLR, 2017, pp. 87–96.
- [18] Texas-Instruments. Introduction to mmwave radar sensing: Fmcw radars. <https://training.ti.com/node/1139153>.
- [19] T. Instruments. Iwr6843isk, 2021. <https://www.ti.com/tool/IWR6843ISK>.
- [20] H. Fan, H. Su, and L. J. Guibas, "A point set generation network for 3d object reconstruction from a single image," in *IEEE CVPR 2017*.
- [21] C. R. Qi, L. Yi, H. Su, and L. J. Guibas, "Pointnet++: Deep hierarchical feature learning on point sets in a metric space," *arXiv preprint arXiv:1706.02413*, 2017.
- [22] A. Kar, C. Häne, and J. Malik, "Learning a multi-view stereo machine," in *Proceedings of the 31st International Conference on Neural Information Processing Systems, 2017*, pp. 364–375.
- [23] D. Paschalidou, O. Ulusoy, C. Schmitt, L. Van Gool, and A. Geiger, "Raynet: Learning volumetric 3d reconstruction with ray potentials," in *IEEE CVPR 2018*.
- [24] M. Ji, J. Gall, H. Zheng, Y. Liu, and L. Fang, "Surfacenet: An end-to-end 3d neural network for multiview stereopsis," in *Proceedings of the IEEE International Conference on Computer Vision, 2017*, pp. 2307–2315.
- [25] J. Wu, C. Zhang, T. Xue, W. T. Freeman, and J. B. Tenenbaum, "Learning a probabilistic latent space of object shapes via 3d generative-adversarial modeling," *arXiv preprint arXiv:1610.07584*, 2016.
- [26] C. Kong, C.-H. Lin, and S. Lucey, "Using locally corresponding cad models for dense 3d reconstructions from a single image," in *IEEE CVPR 2017*.
- [27] N. Wang, Y. Zhang, Z. Li, Y. Fu, W. Liu, and Y.-G. Jiang, "Pixel2mesh: Generating 3d mesh models from single rgb images," in *Proceedings of the European Conference on Computer Vision (ECCV)*, 2018, pp. 52–67.